The 2dF-SDSS LRG and QSO Survey: the star formation histories of luminous red galaxies

Journal Item

The 2dF-SDSS LRG and QSO Survey: the star formation histories of luminous red galaxies

Isaac G. Roseboom,[1]* Kevin A. Pimbblet,[1] Michael J. Drinkwater,[1]
Russell D. Cannon,[2] Roberto De Propris,[3] Alastair C. Edge,[4] Daniel J. Eisenstein,[5]
Robert C. Nichol,[6] Ian Smail,[4] David A. Wake,[7] Joss Bland-Hawthorn,[2]
Terry J. Bridges,[8] Daniel Carson,[6] Matthew Colless,[2] Warrick J. Couch,[9]
Scott M. Croom,[2] Simon P. Driver,[10] Paul C. Hewett,[11] Jon Loveday,[12] Nic Ross,[7]
Donald P. Schneider,[13] Tom Shanks,[7] Robert G. Sharp[2] and Peter Weilbacher[7,14]

[1]*Department of Physics, University of Queensland, QLD 4072, Australia*
[2]*Anglo-Australian Observatory, PO Box 296, Epping, NSW 1710, Australia*
[3]*Cerro Tololo Inter-American Observatory, Casilla 603, La Serena, Chile*
[4]*Institute for Computational Cosmology, Durham University, South Road, Durham DH1 3LE*
[5]*Steward Observatory, 933 North Cherry Avenue, Tucson, AZ 85721, USA*
[6]*Institute of Cosmology and Gravitation, University of Portsmouth, Portsmouth PO1 2EG*
[7]*Department of Physics, Durham University, South Road, Durham DH1 3LE*
[8]*Physics Department, Queen's University, Kingston, ON K7L 3N6, Canada*
[9]*Department of Astrophysics, University of New South Wales, Sydney, NSW 2052, Australia*
[10]*Research School of Astronomy and Astrophysics, Australian National University, Canberra, ACT 2600, Australia*
[11]*Institute of Astronomy, Madingley Road, Cambridge CB3 0HA*
[12]*Dept of Physics & Astronomy, University of Sussex, Falmer, Brighton BN1 9QH*
[13]*Department of Astronomy and Astrophysics, The Pennsylvania State University, University Park, PA 16802, USA*
[14]*Astrophysikalisches Institut Potsdam, An der Sternwarte 16, D-14482 Potsdam, Germany*

ABSTRACT

We present a detailed investigation into the recent star formation histories of 5697 luminous red galaxies (LRGs) based on the Hδ (4101 Å), and [O II] (3727 Å) lines and the D4000 index. LRGs are luminous ($L > 3L^*$) galaxies which have been selected to have photometric properties consistent with an old, passively evolving stellar population. For this study, we utilize LRGs from the recently completed 2dF-SDSS LRG and QSO Survey (2SLAQ). Equivalent widths of the Hδ and [O II] lines are measured and used to define three spectral types, those with only strong Hδ absorption (k+a), those with strong [O II] in emission (em) and those with both (em+a). All other LRGs are considered to have passive star formation histories. The vast majority of LRGs are found to be passive ($\sim$80 per cent); however, significant numbers of k+a (2.7 per cent), em+a (1.2 per cent) and em LRGs (8.6 per cent) are identified. An investigation into the redshift dependence of the fractions is also performed. A sample of SDSS MAIN galaxies with colours and luminosities consistent with the 2SLAQ LRGs is selected to provide a low-redshift comparison. While the em and em+a fractions are consistent with the low-redshift SDSS sample, the fraction of k+a LRGs is found to increase significantly with redshift. This result is interpreted as an indication of an increasing amount of recent star formation activity in LRGs with redshift. By considering the expected lifetime of the k+a phase, the number of LRGs which will undergo a k+a phase can be estimated. A crude comparison of this estimate with the predictions from semi-analytic models of galaxy formation shows that the predicted

*E-mail: roseboom@physics.uq.edu.au

level of k+a and em+a activities is not sufficient to reconcile the predicted mass growth for massive early types in a hierarchical merging scenario.

Key words: surveys – galaxies: evolution – galaxies: formation.

1 INTRODUCTION

The widely accepted paradigm for galaxy formation is the hierarchical merger model which dictates that galaxies form via continuous mergers with smaller objects (e.g. Cole et al. 1994). This scenario is a natural consequence of the Λ cold dark matter (ΛCDM) model of structure formation, which has been highly successful in explaining both the observed structure from the large redshift surveys [2dF Galaxy Redshift Survey (2dFGRS), Colless et al. 2001; Sloan Digital Sky Survey (SDSS), Stoughton et al. 2002], and the anisotropy in the cosmic microwave background (Spergel et al. 2003). In the context of this model, one would naively expect the most-massive galaxies to also be the youngest as they have been 'built up' slowly via mergers. However, traditionally, early types are thought to have formed early and rapidly, with a vast amount of observational evidence points supporting this conclusion. The homogeneous nature of massive early-type galaxy properties, such as small scatter in the colour–magnitude relation (CMR) (Visvanathan & Sandage 1977; Bower, Lucey & Ellis 1992; Aragon-Salamanca et al. 1993; Stanford, Eisenhardt & Dickinson 1995; Ellis et al. 1997; Stanford, Eisenhardt & Dickinson 1998; Terlevich, Caldwell & Bower 2001), and the lack of evolution in these relations with redshift (Kodama et al. 1998; van Dokkum & Stanford 2003), is consistent with a scenario in which most, if not all massive early types, formed at high redshift (at least $z > 2$) and have experienced only passive evolution of their stellar populations since.

While this could simply be a result of selection bias (van Dokkum & Franx 2001), the lack of direct evidence of strong evolution in the population of early-type galaxies since $z \sim 1$ remains a serious problem for the hierarchical model of galaxy formation. In recent years, much work has gone into reconciling these differences. While theoretical models have moved towards consistency with the CMR and fundamental plane (Kauffmann & Charlot 1998; De Lucia et al. 2006, among others), observational studies based on the spectroscopic and morphological properties of early types have found significant populations which show evidence for recent star formation and/or interactions. A morphologically based study by Michard & Prugniel (2004) found that a significant number ($\sim$30 per cent) of nearby ($z \sim 0.01$) early-type galaxies showed evidence of recent interactions/mergers, although 40 per cent of these showed no evidence for a young stellar population. A similar study of 86 nearby bulge-dominated red galaxies by van Dokkum (2005) found that 71 per cent had evidence of tidal interactions. However, given that both these studies were undertaken at low redshift, the volume sampled was too small for significant numbers of LRG analogues to be present. Moving to higher redshifts, Willis et al. (2002) found evidence for current star formation, in the form of detection of the [O II] emission line, in over 20 per cent of a sample of 415 luminous field early types at $z \sim 0.3$. While these studies show that evolution is occurring in at least some of the early-type population, it remains unclear if all early types have experienced evolution of this type. Another contentious point is whether early-type galaxy acquires mass predominately in the form of star-forming gas or already formed stars via so called 'dry mergers' (Bell et al. 2006a).

In this study, we look for evidence of recent star formation in a sample of luminous red galaxies (LRGs). LRGs are luminous ($L > 3L^*$) early-type galaxies, analogous to bright cluster galaxies (BCGs), selected via their red colours which are broadly consistent with a passively evolving stellar population. These galaxies are ideal candidates for the purposes of this study as they have been shown to have relatively homogeneous spectral properties (Eisenstein et al. 2001), enabling any deviation due to recent star formation episodes to be readily identified. They are also the most-massive galaxies, which, if the hierarchical merger model is to be correct, must also have the most vigorous merger histories. Thus, a sufficiently large sample of LRGs provides the perfect test bed for current theories of galaxy formation/evolution.

Here, we probe the star formation histories of our LRG sample via their spectral properties, in particular, the [O II](3727 Å) emission and Hδ(4101 Å) absorption lines and the D4000 index. LRGs are selected from both the SDSS and the 2dF-SDSS LRG and QSO (2SLAQ) surveys, resulting in a sample of 5697 LRGs covering a redshift range of $0.2 < z < 0.7$. Details of the sample selection are presented in Section 2. Section 3 describes the analysis and modelling performed, with the subsequent results presented in Section 4. The implications and conclusions to be drawn from these results are then presented in Sections 5 and 6, respectively.

Where necessary, we have assumed a flat cosmology with $\Omega_m = 0.3$, $\Omega_\Lambda = 0.7$ and $H_0 = 70$ km s^{-1} Mpc^{-1}.

2 THE 2SLAQ LRG SURVEY

Completed in 2005 August, the 2SLAQ survey has collected spectra and measured redshifts for over 10 000 high-redshift QSOs and $\sim$14 000 LRGs in the redshift range $0.45 < z < 0.8$. The survey is essentially a high-redshift extension to the SDSS LRG survey, utilizing the 2dF facility on the Anglo-Australian Telescope to go deeper than that which was possible with the SDSS survey telescope. The 2SLAQ data set has already been utilized to produce photometric redshifts (Padmanabhan et al. 2005), and a large photo-z LRG catalogue (Collister et al. 2006), as well as probe the evolution of the LRG luminosity function from $z = 0.2$ to 0.55 (Wake et al. 2006).

While a detailed description of the survey is presented in Cannon et al. (2006), we briefly review the pertinent points here. The 2SLAQ survey was designed to be an extension of the SDSS LRG survey which sampled LRGs in the redshift range $0.15 < z < 0.5$, to higher redshifts (Eisenstein et al. 2001). The SDSS LRG survey utilized two colour selections in $g - r$ and $r - i$ colour space. One colour selection was used to sample LRGs at redshifts less than 0.4 (cut I), where the 4000-Å break features prominently in the g band, while another (cut II) was used for higher redshifts, where the 4000-Å break is located in the r band. The two cuts were necessary as the 4000-Å break dominates the colour evolution of massive early-type galaxies, such as LRGs, and as such the transition from one band to another causes the track taken by the galaxy in colour–colour space to change considerably. In addition to the colour cut, a sliding magnitude limit was utilized for the low-redshift cut I LRGs as the colours of LRGs at $z < 0.4$ are quite similar to less-luminous
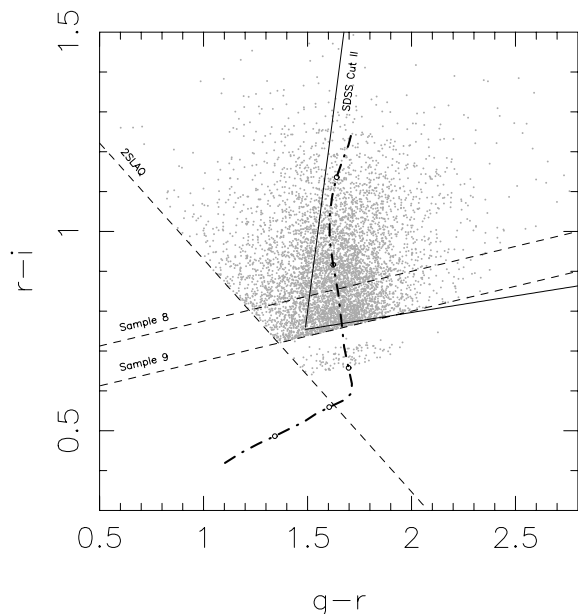
Figure 1. Colour–colour diagram for LRGs selected in this study. The solid lines show the region selected by the SDSS cut II, the dashed lines represent the 2SLAQ selections. The dot–dashed line shows the track taken by a passively evolving early-type galaxy model. The circles are located at $\Delta z = 0.1$ intervals, starting at $z = 0.2$ (lower left-hand panel) and ending at $z = 0.6$ (top right-hand panel). The sharp bend in the track near $z = 0.4$ occurs where the 4000-Å break goes from the g to the r band.

star-forming galaxies at lower redshifts. The 2SLAQ survey utilized a colour selection similar to the higher-redshift, cut II, SDSS colour cut with some key differences. As the number of fibres available to the 2SLAQ survey per square degree was significantly different ($\sim$67 per square degree for the 2SLAQ as compared to only $\sim$2 per square degree for SDSS cut II targets), the colour selection has to be 'loosened' to provide enough targets to fill a 2dF field. This can be seen in Fig. 1 which shows the position of the 2SLAQ LRGs used in this study with respect to both the 2SLAQ and the SDSS cut II colour cuts. A passive evolution track, provided by Bruzual & Charlot (2003) models, is shown as the solid dashed line. The SDSS LRG survey, with its smaller number of targets per field, cuts very close to the passive evolution track and thus goes close to only selecting 'red and dead', passively evolving galaxies. In contrast, the increased availability of fibres from 2dF allows the 2SLAQ selection to be quite broad in $g - r$ colour. This has a distinct advantage over the SDSS in that LRGs with a range of star formation histories are allowed by the 2SLAQ selection, not just strictly passive evolution. In addition to the colour cuts, a magnitude limit of $i_{\mathrm{Dev}} < 19.8$ is imposed so as to ensure that reasonable signal-to-noise ratio (S/N) ($\sim$3) could be achieved in 4 h.

Another key difference between the 2SLAQ and SDSS cut II selections is the grouping and prioritization of targets based on a number of colour cuts. LRGs which lie above the line marked 'Sample 8' were the main goal of the 2SLAQ survey and given the highest priority in targetting. The jump in $r - i$ from the SDSS cut II selection and the 2SLAQ Sample 8 cut is a result of the desire to acquire distinctly higher-redshift LRGs than those present in the SDSS. Sample 9 LRGs were given lower priority and are essentially lower-redshift targets closer to the redshift range of the SDSS cut II LRGs. As sufficient Sample 8 and 9 targets were not necessarily available in each 2SLAQ field, a small number of 'fibre-fillers'

were selected below the Sample 9 cut. These are even lower-redshift LRGs in the region sampled by SDSS cut I.

The 2SLAQ observations were performed using exclusively the 2dF spectrograph 2 with a 600 lines mm^{-1} V grating. This gives a dispersion of 2.2 Å pixel^{-1} and a resolution of about 5 Å. The detector used was a Tek1024 CCD with 1024 × 1024 pixels. Thus, using a 6150 Å central wavelength, the resulting spectra have a wavelength coverage from 5050 to 7250 Å. This coverage was chosen to ensure that the Ca H&K lines were always present in the spectra across the target redshift range of the survey.

In this study, we select 2SLAQ LRGs which fall into the Sample 8 and Sample 9 selections. In addition, only LRGs which have confident redshifts are selected by requiring the redshift quality flag to be greater than or equal to 3. Quality flags on 2SLAQ LRGs are set by the redshift code ZCODE, a derivative of the code used to determine redshifts for the 2dFGRS survey. A quality flag of 3 or greater indicates a high level of confidence in the stated redshift (see Cannon et al. 2006 for details).

We also require that both the [O II] and the Hδ lines are within the wavelength coverage of the spectra and that neither line is in close proximity to the strong sky emission lines at 5577, 5900, 6300 and 7244 Å. The S/N per pixel, averaged across the spectrum, is also required to exceed 3.5 as it was found that lower S/N data produce too many false line detections, as will be discussed in Section 4.1

These requirements bring the number of 2SLAQ LRGs utilized in this study to 5697. It should be noted that all magnitudes and colours throughout are on the ABmag scale, in line with the five-band SDSS photometric system (see Fukugita et al. 1996).

3 METHODOLOGY

3.1 Measuring equivalent widths

Equivalent widths (EWs) of known spectral features are measured using a pseudo-Lick passband flux adding approach. The flux in a set band around the known line wavelength is computed and compared to a continuum level. The continuum is derived by calculating the average flux level in two sidebands and interpolating across the region of interest using these values. For the Hδ and Hγ lines, we use the Lick standard Hδ$_A$ and Hγ$_A$ definition for the passband and sidebands (Worthey & Ottaviani 1997), while for the [O II] line we use the definition from Balogh et al. (1999). These definitions are presented in Table 2. It should be noted that the passband definitions for the absorption lines are the same as those used in the output from Bruzual & Charlot (2003) models. Note that throughout this paper we define a negative EW as emission and a positive value as absorption in a stated line.

D4000 break strengths are also measured for each spectrum in the sample. We define the D4000 index as per Balogh et al. (1999), namely the ratio of the flux in two 100-Å windows centred on 4050 and 3900 Å. While the 2SLAQ spectra are not flux calibrated, we find that the change in spectrograph response is insignificant compared to the intrinsic error in the spectrum and thus the D4000 indices are unaffected.

Errors on the EWs are calculated utilizing equation A8 from Bohlin et al. (1983). Errors in the continuum are based on the standard error in the mean of the sideband flux; errors in the line are based on variance spectrum calculated by the 2DFDR pipeline. It should be noted that while the EW, and D4000, errors take into account 'random' errors such as photon counting statistics, they do not include contributions from systematic errors in the spectra, such as poor sky-subtraction or flat-fielding. Contributions from these

Table 1. EWs and D4000 indices for all the 2SLAQ LRGs used in this paper.

Object name	Redshift	$g - r$	$r - i$	i mag	EW([O II])	ΔEW([O II])	EW(Hδ)	ΔEW(Hδ)	D4000	ΔD4000
J233021.92−002219.5	0.6126	1.0711	1.1299	20.0179	8.8380	0.39	2.3880	0.28	1.5210	0.0135
J233008.15−000142.9	0.6518	1.1798	0.9388	19.8406	9.3080	0.31	−3.3810	0.20	1.2570	0.0132
J232956.99−000423.9	0.6240	2.0150	1.1624	20.0953	4.1390	0.32	3.6820	0.20	1.6620	0.0135
J232955.43−000926.7	0.6064	1.1194	0.9245	19.5885	1.5140	0.27	−1.7250	0.21	1.2260	0.0135
J232952.49−003539.1	0.6027	1.1920	0.9834	20.0139	3.3160	0.38	1.3330	0.27	1.3340	0.0137
. . .										
. . .										

sources to the EW measure could be as high as a few per cent, and as such the quoted errors are likely underestimates of the true error. While this may be of concern for future users of the data presented in Table 1, this is not considered a problem here as the error on the indices does not play a major role in any of the results presented.

A listing of the EW measures on the [O II] and Hδ line, as well as the D4000 indices for all 5697 2SLAQ LRGs used in this study can be found in Table 1.

4 RESULTS

4.1 Definitions based on [O II] and Hδ

In this section, we present a number of spectral classifications based on the [O II] and Hδ EWs which will be used in the subsequent analysis. We split the LRGs into four categories based on their position in the Hδ–EW([O II]) space.

(i) Passive – LRGs with no significant [O II] emission [EW([O II]) > −8 Å] or Hδ absorption [EW(Hδ) < 2 Å], indicating an old passively evolving stellar population.

(ii) k+a – LRGs with significant Hδ absorption [EW(Hδ) > 2 Å] but no [O II] emission [EW([O II]) > −8 Å].

(iii) em – LRGs with significant [O II] emission [EW([O II]) < −8 Å] but no Hδ absorption [EW(Hδ) > 2 Å].

(iv) em+a – LRGs with significant Hδ absorption [EW(Hδ) > 2 Å] and significant [O II] emission [EW([O II])>2 Å].

The implementation of this classification scheme quantitatively involves a careful determination of what a 'significant' amount of [O II] emission or Hδ absorption is in light of the quality of the data set. Physically, the divisions in the EW(Hδ)–EW([O II]) space should be designed in such a way so as to isolate LRGs which have star formation histories that are distinctly different from simply passive evolution. In the high S/N, and resolution limit, this is relatively easy as passive evolution models have no [O II] emission and low levels of Hδ. However, in the low-S/N, low-resolution regime, in which the 2SLAQ LRG spectra predominately lie, variations in the EW(Hδ) and EW([O II]) will be dominated by noise rather than

intrinsic physical properties. Thus, rather than using a physical justification for our EW(Hδ) and EW([O II]) divisions, we calculate threshold values at which it is unlikely that an LRG has a spectrum of a passively evolving stellar population in the presence of noise.

To achieve this, we introduce 'mock' Hδ and [O II] passbands into our EW analysis. The wavelengths of these 'mock' passbands are positioned in quiet regions of the LRG spectrum away from known spectral lines such that any significant EW measures will be purely a result of noise. The passbands and sidebands used in the mock analysis are found in Table 2. For each spectrum in the 2SLAQ LRG sample, the EW of the 'mock' line index is measured using the method described in Section 3.1. As well as giving us a benchmark with which to determine the optimum EW(Hδ) and EW([O II]) threshold values, this analysis has the advantage that for any arbitrary set of EW(Hδ) and EW([O II]) thresholds, we have a good estimate for the false detection rate, that is, the number of LRGs we expect to fall into our k+a, em+a or em sample due simply to noise.

Fig. 2 shows the distribution of [O II] and Hδ EWs for both the real and the mock index definitions. Note again that negative EWs indicate emission, while positive EWs indicate absorption. The low S/N of the 2SLAQ data is apparent in the spread of the mock EWs for both lines. The distribution of mock EWs covers the same range as the real EWs for both Hδ and [O II], meaning it is impossible to define any divisions which will eliminate all false positives. Thus, we try and define divisions that will minimize the number of false positives while still selecting a statistically significant number of LRGs in each of our classifications. It can be seen that the Hδ mock EW distribution drops significantly at ∼2 Å, creating a large difference between the real and mock distributions. If we use this value to define 'significant' Hδ absorption, the number of combined false positives in the k+a and em+a categories is 102, while the number of LRGs with real EW(Hδ) > 2 Å is 330. Thus, using a division at EW(Hδ) = 2 Å results in 30.1 per cent of k+a and em+a samples being false positives. If we decrease the division to 1 Å, the ratio of false positives to real detections increases to 33.5 per cent, while increasing the threshold to 5 Å only decreases the ratio to 29.9 per cent,

Table 2. Passbands and side continuum bands used to measure the mock Hδ and mock [O II] EWs.

Index	Line passband (Å)	Blue continuum sideband (Å)	Red continuum sideband (Å)
Hδ	4083.5–4122.25	4041.6–4079.75	4128.5–4161.0
[O II]	3713–3741	3653–3713	3741–3801
Hγ	4319.75–4363.5	4283.5–4319.75	4367.25–4419.75
Mock Hδ	4230.5–4242.25	4165.6–4199.75	4245.5–4271.0
Mock [O II]	3590.0–3617	3480.0–3550.0	3617.0–3641.0
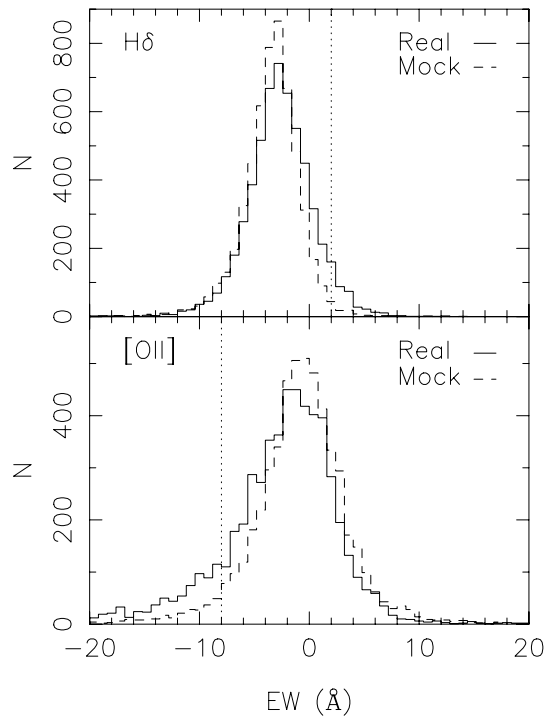
Figure 2. Distribution of real Hδ (top panel) and [O II] (bottom panel) EWs (solid line) and mock Hδ (top panel) and [O II] (bottom panel) EWs (dashed line). The low S/N of the 2SLAQ spectra is apparent from this figure as the mock EW distributions cover a range similar to that of the real EW distributions, despite the fact that there should be no strong features in the passband regions in the mock analysis. The dotted lines show the EW thresholds which define the classification scheme used throughout this paper.

hardly worth a decrease in the number of real detections by 275 (600 per cent).

By a similar justification, we define the EW([O II]) division. The distribution of mock [O II] EWs is seen to drop significantly at ~ -8 Å. Using this value as our EW([O II]) division gives a false positive to real detection ratio of 43.4 per cent. Decreasing to -5 Å gives a ratio of 52.7 per cent, while increasing to -20 Å gives a ratio of 54.9 per cent.

4.2 Spectral properties of 2SLAQ LRGs

Using the selection criteria outlined in the preceding section, we can determine the fraction of LRGs in each of the four categories. Table 1 shows the number of galaxies in each category, and what fraction of the total population they constitute.

Errors on the stated fractions are calculated assuming Poisson statistics.

The corrected fractions are calculated by subtracting the estimated false detection rate calculated in Section 4.1 from the measured

fraction. The false detection rates for the Hδ and [O II] line are transformed into rates for the k+a, em+a and em classifications by assuming that the false detection rate for a line is spread evenly over the classifications requiring it. For example, 30.1 per cent of Hδ detections in k+a and em+a LRGs are false detections, thus if they are spread evenly across both classifications the false detection rate in k+a and em+a LRGs (due to only Hδ) is 20.8 and 9.3 per cent, respectively. In the case of the em+a classification, we define the false detection rate to be the sum of the false detection rates from both Hδ and [O II].

The efficiency of the selection method in isolating passively evolving ellipticals is again apparent from Table 3 with over 80 per cent of LRGs having the spectral features indicative of an old passively evolving stellar population.

A number of example spectra for each of the spectral classes are shown in Fig. 3. Spectral features discussed are marked. It can be seen that in the spectra with strong Hδ, the other, higher-order, Balmer lines are also observed.

The combined spectra for each spectral type are presented in Fig. 4. The combined spectra are produced by first de-redshifting each spectrum, and rebinning to a common dispersion. The spectra are first normalized using the mean flux in a 100-Å window (4000–4100 Å). The top and bottom 10 per cent of values at each pixel are then excluded. The mean of the remaining values at each pixel is then used to produce the combined spectrum. For each combined spectrum, the D4000 index and EWs of the Hδ, Hγ, Hβ and [O II] lines have been measured using the methods presented in Section 3.1, with the results presented in Table 1.

While it is generally accepted that Hδ is an efficient indicator of a young stellar population, the presence of strong Hδ absorption should be accompanied by increased absorption in the other Balmer lines. To test this, we measure the EW of the Hγ line in the combined spectra, with the results presented in Table 3. Hγ alone is utilized as the lower-order Balmer lines (Hβ, Hα) are not inside the wavelength coverage of many of the higher-redshift spectra. It can be seen that for classifications which pass the EW(Hδ) > 2 Å cut, k+a and em+a, the EW of Hγ is significantly greater in absorption than that found in the passive combined spectrum. It should be noted that the Hγ EWs quoted in Table 1 appear to be in emission (i.e. negative) as emission in the nearby passbands used to estimate the continuum dominates moderately low levels of absorption in the line itself. The ratio of the calcium H to K lines is also notably greater in the k+a and em+a combined spectrum than that in the passive spectrum (Fig. 4). This can be attributed to increased absorption in the Hε line, which is coincident with the calcium H line. Thus, we can be satisfied that our selection based on Hδ alone has been effective in isolating LRGs with overall increased Balmer line absorption, and hence potentially younger stellar populations.

Fig. 5 shows the D4000 distributions for the k+a (bottom panel), em+a (middle panel) and em (top panel) spectral classifications. The whole 2SLAQ sample is designated by the solid line, while the D4000 distribution of only the passive LRGs is shown by the
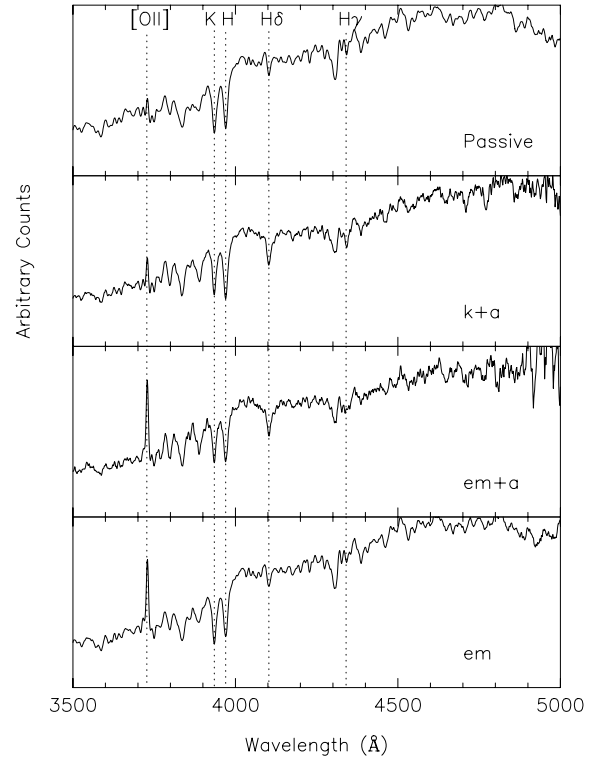
Table 3. Fraction of each spectral type and properties of their combined spectrum.

Spectral type	Number	Fraction (per cent)	Corrected fraction (per cent)	D4000	EW([O II]) (Å)	Hδ (Å)	EW(Hγ) (Å)
Passive	4612	81 ± 1	88 ± 1	1.75 ± 0.01	-1.0 ± 0.1	-1.67 ± 0.08	-5.83 ± 0.08
k+a	225	3.9 ± 0.3	2.7 ± 0.2	1.53 ± 0.01	-2.3 ± 0.1	3.7 ± 0.1	-1.7 ± 0.01
em+a	101	1.8 ± 0.2	1.2 ± 0.1	1.50 ± 0.01	-12.1 ± 0.1	3.9 ± 0.1	-1.6 ± 0.1
em	759	13.3 ± 0.5	8.6 ± 0.4	1.71 ± 0.01	-11.7 ± 0.1	-1.37 ± 0.09	-5.53 ± 0.08
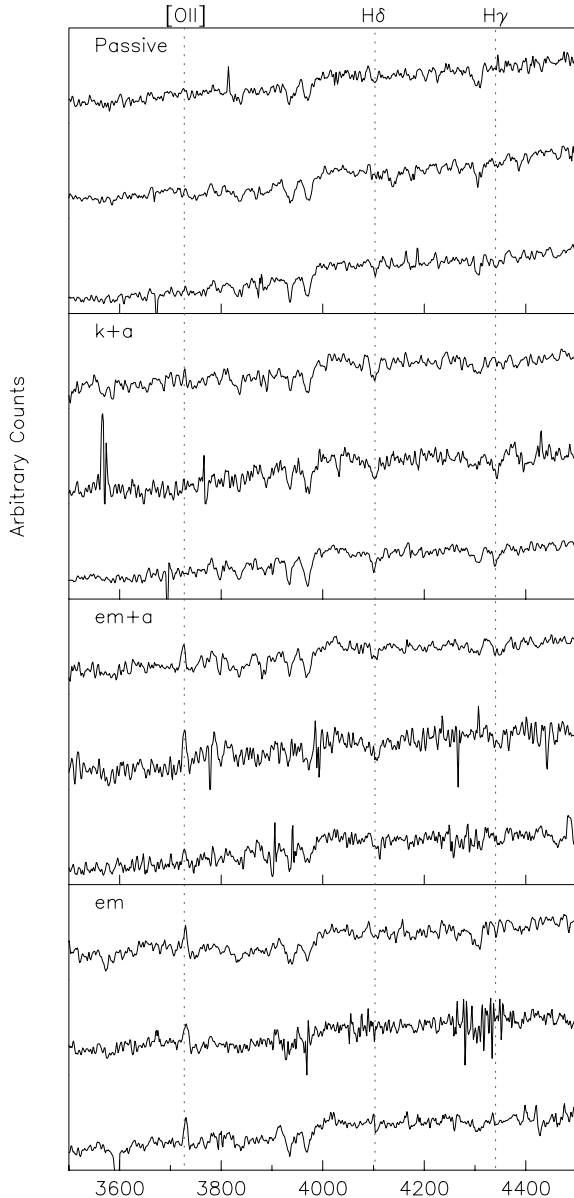
Figure 3. Example spectra for the k+a (top three panels), em+a (middle three panels) and em (bottom three panels) spectral classifications. Spectra have been converted to rest-frame wavelengths, and smoothed by a Gaussian with full width at half-maximum (FWHM) = 0.84 Å. Spectral features discussed in the text are marked.


Figure 4. Combined spectrum for the four spectral classifications. Quantities measured on the spectra are presented in Table 1. Note the increase in the absorption strength of the higher-order Balmer lines (Hγ, Hε, etc) in the k/em+a combined spectra.

dashed line. The D4000 index is well known to be sensitive to recent star formation, with lower values indicating the increasing presence of a young A star population. As expected, the D4000 indices for LRGs in the 2SLAQ sample suspected to have recent star formation, (k+a and em+a) are notably less than that for the passively evolving LRGs. The em+a LRGs also show significantly lower D4000 indices than the k+a LRGs suggesting that the em+a galaxies have experienced more recent, or ongoing, given the presence of the [O II] line, star formation. Interestingly, the em LRGs have D4000 indices which are broadly consistent with the passive LRGs. While a Kolmogorov–Smirnov (KS) test shows that all three distributions are statistically inconsistent with the passive population, with p-values of 2.4×10^{-6}, 2.6×10^{-17} and 6.6×10^{-22} for the em, em+a and k+a LRGs, respectively, a significant fraction of the

em LRG population are found to have D4000 indices as large as those found in the passive population. This is in stark contrast to the k+a and em+a LRG populations which are very rarely found at high D4000 index (i.e. D4000 > 2). This would suggest that while recent star formation is unambiguously responsible for k+a and em+a LRGs, the origins of em LRG population are not so clear.

4.3 Redshift dependence

To test the redshift dependence of the classification fractions, the 2SLAQ LRGs are divided into two subsamples between $0.45 < z < 0.55$ and $0.55 < z < 0.65$. In order to increase the redshift range of the analysis, a low-redshift sample for comparison is provided by SDSS MAIN survey galaxies with $0.1 < z < 0.2$. While the SDSS also conducted an LRG survey, the selection criteria for SDSS LRGs are much stricter than those for the 2SLAQ, so strict that only ~700 2SLAQ LRGs would be selected in the SDSS survey at $z = 0.2$. It is for this reason that we utilize galaxies from the SDSS MAIN survey for comparison.

As the 2SLAQ LRGs were selected by an observed-frame colour selection, some effort must be made to ensure that our comparative sample from SDSS is consistent with the colour selections of the 2SLAQ. Indeed, effort must also be made to ensure that the colour selections are consistent within the redshift range covered by the 2SLAQ itself. The simplest way to accomplish this is to use an independent rest-frame selection in the colour–magnitude space on both the 2SLAQ and the SDSS MAIN galaxies. To determine the appropriate boundaries of this selection, we present the M_i and rest-frame $g - i$ evolution of the 2SLAQ galaxies with redshift in Fig. 6. Absolute magnitudes for the 2SLAQ galaxies are produced via the
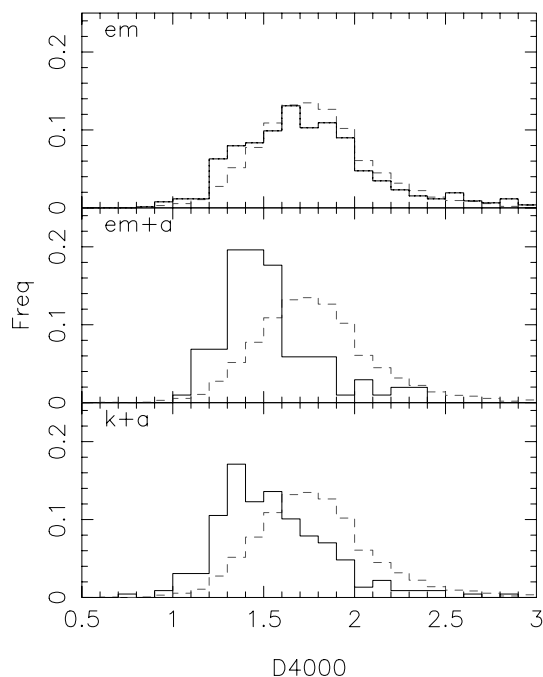
Figure 5. Distribution of D4000 indices for k+a (bottom panel), em+a (middle panel) and em (top panel) LRGs. In each case, the distribution is marked with a solid line, while the distribution of passive LRGs is marked with a dashed line. The k+a and em+a LRGs show systemically lower D4000 indices than the passive LRGs. This, along with their increased Hδ, confirms the presence of a younger stellar population in these LRGs. Significant numbers of em LRGs show D4000 strengths that are as large as those found in the passive population, suggesting that a large fraction of em LRGs do not possess significant populations of young stars.

use of model k+e corrections based on Bruzual & Charlot (2003, henceforth BC03) models. The models assume simple passive evolution of the stellar population from a single epoch of high redshift star formation. This sort of model has been found to approximate the colour evolution of LRGs to ~0.1 mag (Wake et al. 2006), which is satisfactory for our purposes here. While ideally k-corrections could be derived directly from the spectra, the 2SLAQ spectra are not flux-calibrated, nor do they have the significant wavelength coverage required for such calculations. Significant redshift evolution is shown in both the $g - i$ colour and the M_i of the LRGs in Fig. 6. The M_i evolution is a result of the $i_{\mathrm{Dev}} < 19.8$ magnitude limit of the 2SLAQ survey, while the increase in the distribution of $g - i$ colours to bluer values is a result of the colour selection becoming 'looser' at higher redshifts (as can be seen to some extent in Fig. 1). It can be seen that a cut at $g - i > 0.8$ (as shown by the dashed line) will produce a sample which is reasonably consistent in colour with redshift. Similarly, a cut at $M_i < -22$ will produce a sample which is close to volume-limited. It is on this cut-down 'homogeneous' sample of 2SLAQ LRGs that the following analysis is performed.

In a similar fashion, we select galaxies from the SDSS MAIN survey which have rest-frame $g - i > 0.9$ and $M_i < -22.0$. As the SDSS spectra have a wide wavelength coverage, and good spectrophotometric calibration, k-corrections can be derived directly from the spectra. This has been done for the DR4 MAIN galaxies by Blanton et al. (2005) and can be found in the NYU SDSS value-added catalogue (VAC) available at http://wassup.physics.nyu.edu/vagc/. k-corrections in the NYU VAC are produced via the use of the KCOR-RECT software (v3.4) described in Blanton et al. (2003). As the VAC
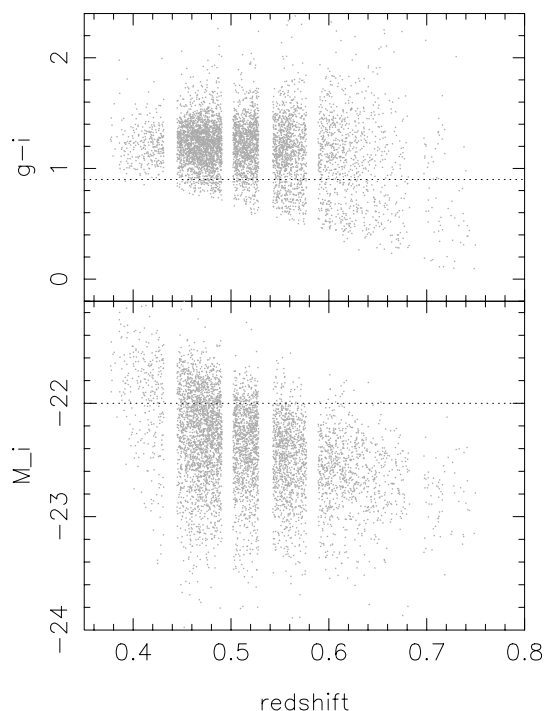
Figure 6. Rest-frame $g - i$ and M_i redshift evolution for the 2SLAQ LRGs. Rest-frame quantities are produced via k+e corrections based on a BC03 model track. The model assumes a single epoch of star formation for the LRG stellar population at high redshift, followed by passive evolution. The dashed line shows the cuts utilized in the text to produce a sample of LRGs which are unbiased in colour and luminosity with redshift.

only provides k-corrected photometry, the M_i cut is adjusted slightly to -22.2 to take into account the M_i evolution from $z = 0$ to 0.15 predicted by the BC03 models used to $k + e$-correct the 2SLAQ LRGs.

The results of this analysis are presented in Fig. 7 and Table 4. In each subsample from the 2SLAQ, and for the low-z SDSS galaxies, we calculate the number of each spectral classification present, and the fraction of the bin that this number constitutes. Errors are again calculated assuming Poisson statistics. Since the LRGs are not uniformly distributed inside each bin, the bin centres are taken to be the median redshift of all the LRGs in a given bin.

In order to correct for the occurrence of false detections, we again apply corrections to the fractions estimated using the results of the 'mock' line analysis from Section 4.1. By dividing the 'mock' EW measures on Hδ and [O II] into the same redshift bins as the real analysis, we produce corrections which are indicative of the underlying S/N distribution in each bin. This has the advantage of also eliminating any possible bias that may arise from varying S/N across the redshift range.

The raw and corrected fractions are presented in Fig. 7 with the values shown in Table 4.

The effect of the $g - i > 0.9$ and $M_i < -22$ cuts on the number of k+a and em+a LRGs is quite dramatic. Only 79 out of the original 225 k+a LRGs and even more dramatically only 23 out of the original 101 em+a LRGs pass the cuts. However, this is not all that surprising, given the strong correspondence between k+a and em+a features and low D4000, which can be taken as an effective proxy for $g - i$ colour.

It can be seen from Fig. 7 that only the k+a LRG fraction shows a clear trend of increasing with redshift. The em LRG fraction shows
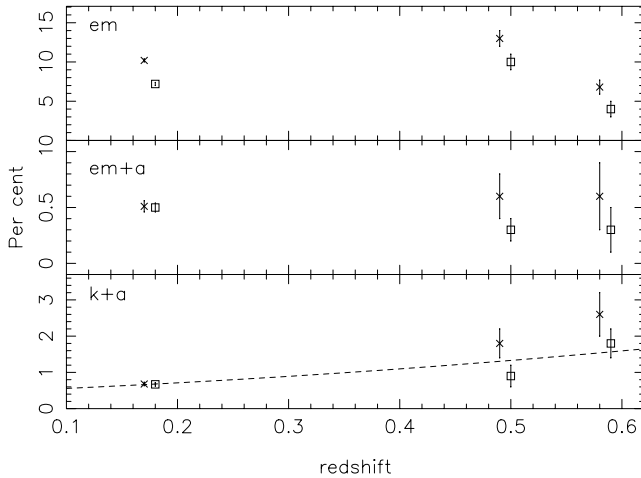
Figure 7. Redshift dependence for the raw (crosses) and corrected (squares) fraction of each classification with redshift. For comparison, the fraction of each classification in a sample of low-redshift ($z \sim 0.15$) SDSS MAIN galaxies is shown. The SDSS MAIN galaxies are required to have the same luminosity and colour range as the 2SLAQ LRGs by placing simple cuts in rest-frame $g - i$ and M_i. While the em and em+a fractions do not show any overall trend with redshift, the k+a fraction shows a strong increase. Fitting a $(1 + z)^n$ relation to the k+a fraction increases gives $n = 2.8 \pm 0.7$. The fit is shown by the dashed line.

a strong increase between the SDSS $z = 0.17$ sample and 2SLAQ LRGs at $z = 0.49$, but then shows a significant drop in the highest-redshift bin. Little can be said about the em+a LRG fraction as the numbers in the 2SLAQ bins are too low.

In order to quantify the redshift dependence of the k+a fraction in Fig. 7(a), $(1 + z)^n$ fit has been performed on the corrected fractions. Fitting is performed via weighted linear regression in $\log(z)$ versus $\log$(fraction) space. The fit is shown by the dashed line in Fig. 7. The k+a fraction is found to obey a $(1 + z)^{2.8 \pm 0.7}$ relation.

5 DISCUSSION

5.1 Comparison with previous work

In recent years, many authors have looked for recent and/or ongoing star formation amongst samples of early-type galaxies. Fukugita et al. (2004) performed a spectroscopic study of 420 E/S0 $z \sim 0.12$ galaxies selected from the SDSS. They found evidence of ongoing star formation, in the form of Hα emission, in 19 (4.5 per cent) and k+a like spectral properties in 15 (3.6 per cent). Yi et al. (2005) also identified early types with recent star formation in the SDSS, this time using GALEX near-ultraviolet (NUV) and SDSS r-band photometry. $\sim$15 per cent of their sample of 39 bright ($M_r < -22$), early-type, $z < 0.13$ galaxies was found to have evidence of recent star formation via the use of NUV $- r$ colour. Moving to higher

redshifts, Doherty et al. (2005) and Le Borgne et al. (2006) both found significant fractions ($\sim$30 and 50 per cent, respectively) of k+a LRGs amongst massive galaxies at $z \sim 1$.

A significant fraction of 2SLAQ LRGs fall into the em category (6.8 ± 0.3 per cent), although this result is not completely unexpected as a study by Willis et al. (2002) found that over 20 per cent of their sample of luminous-field early-type galaxies had significant [O II] emission. Similarly, Eisenstein et al. (2003) found that $\sim$10 per cent of their sample of massive bulge-dominated galaxies had emission-line components.

However, it is difficult to make concrete comparisons between these results and those presented here. This is because the fraction of early types with young stellar populations is very sensitive to the sample selection. This can even be seen here, with significant differences in the fraction of k+a and em+a LRGs between the whole sample in Section 4.2 and cut-down sample used in Section 4.3. Most previous studies, including those discussed above, use a selection based on morphological information. This is distinctly different from the colour-based selection used in the 2SLAQ survey. It should be expected that morphology-based studies of early types will find greater fractions of galaxies with young stellar populations than we find here as the colour selection is strongly biased against the selection of galaxies with large populations of young stars. Thus, while the absolute fractions of k+a and em+a LRGs quoted here are not directly comparable to other work on massive early types, the observed increase with redshift should be consistent between the studies.

This notion is supported not only qualitatively by the jump in the number of 'young' early types between $z \sim 0.1$ and $z \sim 1$ but also quantitatively by a comparison of the measured redshift dependence of the k+a fraction here and in the study of Le Borgne et al. (2006). Le Borgne et al. (2006) performed a study of the spectral properties of massive ($M > 10^{10.02}$ M$_\odot$) galaxies selected from the Gemini Deep Deep Survey (GDDS; see Abraham et al. 2004) and SDSS MAIN galaxy sample. While they did not base their selection on morphology or colour, and hence found a significantly greater number of k+a than we find, they found an evolution of $(1 + z)^{2.5 \pm 0.7}$ across a redshift range of the $0.1 < z < 1.2$. Le Borgne et al. (2006) noted that this value is very close to the predicted evolution of the galaxy merger rate in ΛCDM semi-analytic models of $(1 + z)^{3.2}$ (Le Fèvre et al. 2000). Interestingly, the fraction of k+a and em+a LRGs found here is very close to 4 ± 1 per cent fraction of massive galaxies in close pairs found by Bell et al. (2006b). Thus, if k+a and/or em+a activity is triggered by mergers, the fractions and evolutionary trends we find here are reasonably consistent with other merger indicators in the literature.

5.2 Hδ strong LRGs

If we accept the interpretation that the observed Hδ absorption in the k+a and em+a LRGs is a result of recent star formation, which seems likely, given the weaker D4000 indices and observed
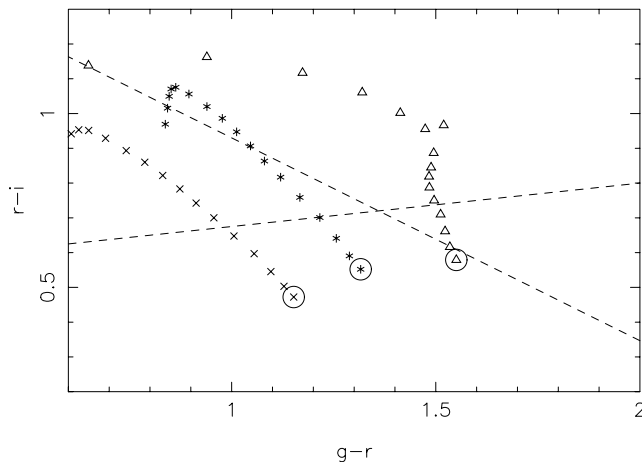
Table 4. Redshift dependence of classification fractions. Quoted errors are calculated assuming Poisson statistics. The fractions are calculated by first producing a truncated sample which is uniform in colour and luminosity with redshift, and then correcting the fractions using the same analysis as described in Section 4.1. The low-redshift $z \sim 0.17$ point is measured using SDSS MAIN galaxies with the same rest-frame colours and luminosities as the 2SLAQ LRGs.

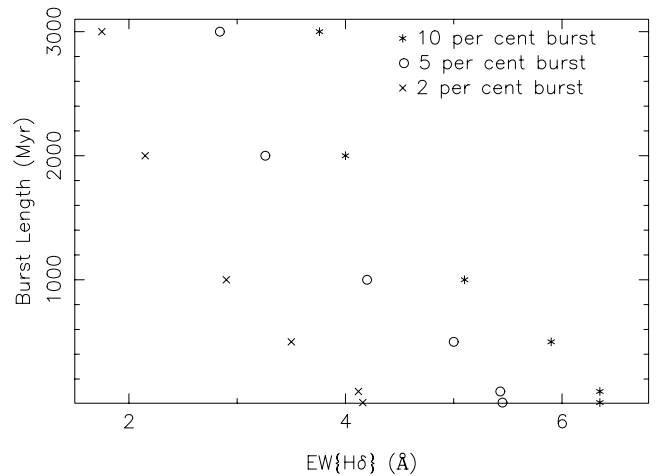| z	N(LRGs)	N(k+a)	Per cent	Corrected	N(em)	Per cent	Corrected	N(em+a)	Per cent	Corrected
0.17	20 781	143	0.68 ± 0.05	0.67 ± 0.05	2115	10.2 ± 0.2	7.2 ± 0.2	107	0.51 ± 0.04	0.50 ± 0.04
0.49	2610	46	1.8 ± 0.4	0.9 ± 0.3	303	13 ± 1	10 ± 1	16	0.6 ± 0.2	0.3 ± 0.1
0.57	1141	33	2.9 ± 0.6	1.8 ± 0.4	78	6.8 ± 0.9	4 ± 1	7	0.6 ± 0.3	0.3 ± 0.2

absorption in the higher-order Balmer lines (see Section 4.2), then a small, but significant, number of the LRG population (∼1 per cent) has been forming stars within the last 2 Gyr. This is an important result as it shows that evolution is occurring in the massive early-type population at redshifts less than 0.7.

To try and quantify the level of star formation required to produce the observed EW(Hδ), we turn to the spectral synthesis models of BC03. A distinct advantage of using these models is that they produce output measurements of the indices discussed here (D4000 and Hδ) measured in the same fashion as outlined in Section 3. All the models presented in this section assume a Salpeter (1955) initial mass function, solar metallicity, and no dust-reddening.

While constant star formation in a galaxy will produce the required level of Hδ, this scenario has two major problems. First k+a LRGs show no [O II] emission, suggesting that there is no ongoing star formation occurring; however, it is possible that the [O II] could be missing due to preferential dust obscuration or even aperture effects. Secondly, models show that galaxies with continuous star formation will mostly be outside the LRG colour selection. Fig. 8 shows model tracks for two constant star formation models and a purely passive evolution model. In each of the constant star formation models, a large fraction of the stellar population is formed at high redshift ($z \sim 3$), with low levels of constant star formation responsible for 10 and 5 per cent of the stars at an age of 10 Gyr. The 10 per cent model track falls well outside the 2SLAQ colour selection, while the 5 per cent model track just enters the 2SLAQ selection at $z > 0.55$. The typical Hδ of the model spectra in the redshift range probed by the 2SLAQ is ∼2.9 and ∼1.6 Å for the

Figure 9. Effect of changing the length of the starburst on the peak EW(Hδ). Bursts consuming 2 (crosses), 5 (circles), and 10 (asterisks) per cent of galactic stellar mass are shown. The peak EW(Hδ) is seen to decrease with increasing burst length. It is likely that the star formation rate, not the total size of the burst, is the dominating factor in determining the peak EW(Hδ).

10 and 5 per cent model, respectively. Thus, the 10 per cent model spectra would be selected in our k+a sample, but not in the 2SLAQ and the 5 per cent model would be selected in the 2SLAQ, but not as a k+a. As the 5 per cent model only just falls into the 2SLAQ selection, we consider it unlikely that continuous star-forming models can explain the k+a LRGs in the 2SLAQ.

Thus, we confine ourselves to models in which a significant episode of star formation has occurred and subsequently ceased. In order to simplify the models, we only consider scenarios in which an instantaneous burst of star formation is superimposed on an old stellar population. While it is likely that star formation histories with longer periods of star formation are responsible for the k/em+a population, the tracks taken by such models after star formation has ceased are nearly indistinguishable from the instantaneous burst models. The only quantitative difference is that longer starburst models require that a larger fraction of the LRG mass be consumed in star formation to achieve the same level of Hδ absorption. This can be seen from Fig. 9 which shows the relationship between burst length, and peak Hδ for models which consume 2, 5, and 10 per cent of galactic stellar mass in new star formation. In all cases, the models superimpose a burst of constant star formation on an old (7.4 Gyr) stellar population. The peak EW(Hδ) is found to be not only dependent on the size of the burst (i.e. the total number of new stars created) but also strongly dependent on the period over which the burst occurs. Indeed, for bursts in the range 500–2000 Myr, the peak EW(Hδ) is dominated by the star formation rate, not the total size of the burst. This can be seen if we take an arbitrary peak EW(Hδ) and look at the star formation rate (in per cent of galactic stellar mass per year) required for the three burst sizes presented in Fig. 9. Using EW(Hδ) = 4 Å as an example, we estimate star formation rates for the 2, 5 and 10 per cent models of 6.6×10^{-9}, 4.2×10^{-9} and 5.0×10^{-9} per cent per year, respectively. It can be seen that these values are in relatively good agreement.

Fig. 10 plots the track taken in the EW(Hδ)–D4000 space by models in which starbursts consuming 1, 2 and 5 per cent of stellar mass have occurred. In each case, the model assumes an instantaneous burst occurs in a passively evolving stellar population which formed 7.4 Gyr before burst. Also shown in Fig. 10 is the number density of LRGs plotted in grey-scale. As expected, a slight trend of increasing

Figure 8. Model $g − r$, $r − i$ tracks for two constant star formation models (crosses and asterisks), and a passive evolution model (triangles). The constant star formation models assume that most of their stars are formed at high redshift, with a low level of constant star formation occurring since. The crosses represent a model in which 90 per cent of the stellar population at an age of 10 Gyr was formed at high redshift, the asterisks represent a model where 95 per cent were formed at high redshift. The dashed line shows the Sample 9 2SLAQ selection described in Section 2. The passive evolution model assumes that all the stars are formed at high redshift, and have experienced only passive evolution since. The circles indicate redshift of $z = 0.4$ and the tracks mark the evolution from z = 0.8 (near the upper left-hand border) to $z = 0.4$ at $\Delta z = 0.025$ intervals. Assuming a formation age of $z = 3$ for the model, the typical Hδ in the redshift range probed by the 2SLAQ is ∼2.9 and ∼1.6 Å for the 10 and 5 per cent model, respectively. Thus, it can be seen that any galaxy experiencing a level of constant star formation high enough to pass our EW(Hδ) > 2 Å cut would not be selected by the 2SLAQ colour selection.

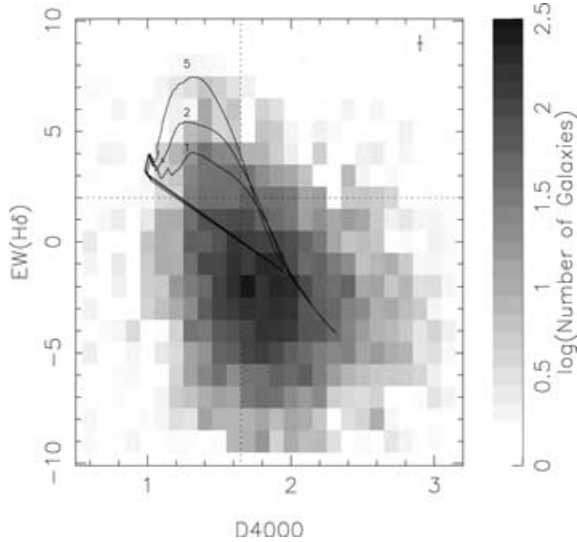**Figure 10.** Number density of LRGs in the D4000–EW(Hδ) plane. The plane is broken down into 0.1 × 1 cells, the grey-scale representing the logarithm of the number of LRGs in the cell. The scale goes from light to dark, with the darkest spot equal to 316 ($10^{2.5}$) LRGs. Also plotted are model tracks for a series of models assuming bursts of star formations consuming 5 (top), 2, and 1 (bottom) per cent of stellar mass in new star formation. Typical errors on both indices are shown in the top right-hand corner. A significant number of LRGs have EW(Hδ) and large D4000 indices which cannot be explained by these simple models. These are analogous to red Hδ-strong galaxies found in the literature (e.g. Couch & Sharples 1987).

EW(Hδ) with decreasing D4000 is observed. Reasonable agreement is found between the Hδ strong LRGs and the model tracks. Given that we have only presented tracks for a limited range of models, it should be possible to produce models in a similar vein to those presented which can match any observed EW(Hδ). However, this is not the case for all values of D4000. The dotted vertical line at D4000 = 1.65 is used to crudely divide between those Hδ strong LRGs which roughly agree with the models and those which do not. Of the 326 Hδ strong LRGs in the 2SLAQ, 98 (30.1 per cent) have D4000 > 1.65. Many of the previous E+A/Hδ-strong studies have also identified a population of red Hδ strong galaxies with photometric properties that are too red to be consistent with models (Couch & Sharples 1987; Poggianti et al. 1999; Blake et al. 2004; Balogh et al. 2005). While dust and supersolar metallicities can be called on to redden the model tracks, and hence explain the discrepancies observed, it has been repeatedly shown that these effects, when used in plausible amounts, can only move the tracks shown in Fig. 10 by at most 0.1 in D4000 (Balogh et al. 1999; Pracy et al. 2005), not nearly enough to explain the reddest Hδ strong LRGs. Curiously, the fraction of red Hδ strong LRGs in the 2SLAQ is exactly equal to the predicted number of false positives in the sample. Given this, it would seem probable that most, if not all, of the red Hδ strong LRGs in this study are simply false detections. If this is true, then the origin of the k+a and em+a LRG populations can be most readily explained by recent bursts of star formation, on the scale of 1 per cent of galactic stellar mass, in otherwise passive LRGs.

5.3 em LRGs

The origin of the em LRGs is more ambiguous as the observed [O II] emission could originate from either ongoing star formation or active galactic nuclei (AGN). Typically, the nature of emission lines in optical spectra can be determined via the use of line ratios (e.g. Baldwin, Phillips & Terlevich 1981), or even more unambiguously by their radio properties. Unfortunately, neither of these diagnostics is readily applicable here. The traditional optical line ratios used for classifying AGN/star formation are Hβ, [O III] 5007 Å, and Hα, all of which have wavelengths too red to appear inside the wavelength coverage of 2SLAQ spectra. Sadler et al. (in preparation) have performed a cross-matching of the 2SLAQ LRGs to radio sources in both the FIRST and the NVSS catalogues. Of the 13 784 2SLAQ LRGs with confident redshifts, only 378 have corresponding radio sources in the FIRST; this is despite the FIRST covering 96.5 per cent of the 2SLAQ survey area. Of the 759 em LRGs found in the sample presented here, only 21 (2.8 per cent) have a FIRST radio detection within 5 arcsec, very close to the overall radio detection rate of 2.7 per cent. Similarly, Sadler et al. (2006) found that the fraction of radio detections with [O II] emission is the same as the fraction in the whole 2SLAQ sample. However, while strong radio continuum emission can unambiguously identify an AGN, the converse, that is, lack of radio emission constitutes a lack of AGN activity, is not true. Thus, while we can be confident that at least 2.8 per cent of em LRGs have AGN, little can be said about the remaining 97.2 per cent from available radio data.

However, despite the lack of data with which to accurately classify each em LRGs, we can muse about the origins of em LRGs. A strong piece of evidence against a star-forming origin for all em LRGs is the lack of correlation between [O II] emission and lower D4000 indices. The D4000 index is very sensitive to any population of young stars, as seen in the case of the k+a and em+a LRGs in Fig. 5. Thus, unless we are observing an LRG during the very short period of time at the very beginning of a star formation episode before substantial numbers of young stars have been formed, their should be a clear relation between the D4000 index and current star formation. However, if the [O II] emission originates from AGN activity, this should have no discernable effect on the D4000 index. Given this, it is unlikely that the large number of em LRGs with relatively large D4000 indices have star-forming origins. However, given the large spread in the D4000 index seen in the passive LRG population (Fig. 5), it is impossible to say whether the em LRGs with low D4000 index are actively star forming.

5.4 Recent star formation in LRGs and the ΛCDM paradigm

Assuming that recent and/or ongoing star formation is the cause of the observed spectral characteristics of the k/em+a LRGs, which is likely, given the arguments of the previous sections, a number of well-known phenomena can be called on as potential candidates for the origin of star formation in LRGs.

Given that LRGs are akin to massive early-type galaxies, a sizeable fraction will reside in groups or clusters, making a small, but significant, number of them bright cluster or even cD galaxies. Thus, it is plausible that these central cluster LRGs may be at the focus of a cooling flow. The presence of optical emission lines in 20–30 per cent of all brightest cluster galaxies in X-ray selected samples has been confirmed in a number of studies (Donahue, Stocke & Gioia 1992; Crawford et al. 1999) and an extreme population of galaxies with massive starbursts (50–200 M$_\odot$ yr^{-1}) has been identified (Allen 1995; Crawford et al. 1999). These galaxies could be the progenitors of the k/em+a LRGs if the starburst is truncated although they would be preferentially found in the brightest LRGs.

Another possibility is that the bursts of star formation are being created as a result of LRG–galaxy mergers or interactions. This ties in well with the idea that LRG evolution is dominated by hierarchical

merging. Indeed in this model, one would naively expect (and indeed it has been shown from *N*-body simulations) that the frequency of mergers would decrease significantly with increasing time (decreasing redshift), which is qualitatively in line with the results demonstrated here.

However, it is difficult to make quantitative assertions about the origin of k/em+a LRGs as it is impossible to determine which of these hypotheses is responsible, if at all. Another complication is the potential for differences between the k+a and em+a classes. Previous studies of traditional k+a and em+a analogues at low redshift have found systematic differences between the two classes, suggesting different formation mechanisms (Balogh et al. 2005).

Regardless of the physical nature of the star formation in LRGs, it is reasonably safe to assume that the star-forming gas is coming from an external origin. This is in agreement with the core principles of ΛCDM cosmology. Results from the current generation of hydrodynamic *N*-body cosmological simulations suggest that the most-massive galaxies increase in mass significantly from $z < 1$ (De Lucia et al. 2006), with the bulk of this increase coming from accretion of intracluster gas, or via mergers with smaller galaxies (Murali et al. 2002). By consideration of the expected time-scale of the k+a signature, we can crudely estimate the number of LRGs affected by k+a activity since $z = 0.8$. Converting the redshifts of the bins used in Section 4.3 into look-back time results in a $0.36 \times t^{0.85\pm0.2}$ dependence, where t is the look-back time in Gyr. By simply integrating, we can use this dependence to estimate the fraction of LRGs which undergo a k+a phase between $0 < z < 0.8$ (or $0 < t < 7$) as 8 per cent. For comparative purposes, we consider both the models of De Lucia et al. (2006) and the observational evidence presented by Bell et al. (2006b). De Lucia et al. (2006) predicted that ∼50 per cent of massive early types gain 50 per cent of their stellar mass between $0 < z < 0.8$. Similarly, Bell et al. (2006b) predicted from their measure of the close pair fraction that ∼20 per cent of massive galaxies will undergo a major merger between $0 < z < 0.8$. Thus, even if k+a, or em+a, activity was associated with a major merger event that doubled the mass of the progenitor LRG, which is unlikely, given the models presented in Section 5.2, this would only account for ∼16 per cent of the required mass growth in massive early types in the models, and only 40 per cent of the predicted number of mergers in massive galaxies from observations. It is clear from this crude comparison that the level of k+a and em+a activities is not sufficient to explain the bulk of the mass growth in massive early types. This is in line with recent results which suggest that red or 'dry' mergers are responsible for the growth of massive early-type galaxies (van Dokkum 2005; Bell et al. 2006a).

6 CONCLUSION

We have determined the recent star formation histories of a sample of 5697 LRGs based on the EWs of the Hδ and [O II] lines. While the majority (>80 per cent) show the spectral properties of an old, passively evolving, stellar population, a significant number of LRGs show evidence for recent and/or ongoing star formation in the form of k+a (2.7 per cent), em+a (1.2 per cent) or em LRGs (8.6 per cent). By dividing the sample into two redshift subsamples from $0.45 < z < 0.55$ and $0.55 < z < 0.65$, and comparing to a $z \sim 0.15$ sample selected from SDSS, it is observed that the fraction of k+a LRGs increases with redshift as $(1 + z)^{2.8\pm0.7}$.

Spectral synthesis models, utilizing the code of BC03, suggest that the k/em+a LRGs could originate from passive LRGs which undergo a starburst in which material equivalent to ∼1 per cent of the stellar mass is consumed in new star formation.

Several origins for k+a and em+a LRGs are considered, including cooling flows and mergers; however, identification of the exact formation mechanism, or even if k+a and em+a LRGs share a common origin, is not possible with the current data. It is clear that k+a and em+a activities represent a signpost of recent evolution in LRGs; however, by considering the lifetime of the k+a/em+a phase, we estimate that only 8 per cent of LRGs will experience a k+a or em+a phase between $z = 0.8$ and the present. By comparing this with the semi-analytic galaxy formation models of De Lucia et al. (2006), we conclude that k+a/em+a activity cannot be responsible for the predicted mass growth of massive ellipticals since $z = 0.8$.

REFERENCES

Abraham R. G. et al., 2004, AJ, 127, 2455
Allen S. W., 1995, MNRAS, 276, 947
Aragon-Salamanca A., Ellis R. S., Couch W. J., Carter D., 1993, MNRAS, 262, 764
Baldwin J. A., Phillips M. M., Terlevich R., 1981, PASP, 93, 5
Balogh M. L., Morris S. L., Yee H. K. C., Carlberg R. G., Ellingson E., 1999, ApJ, 527, 54
Balogh M. L., Miller C., Nichol R., Zabludoff A., Goto T., 2005, MNRAS, 360, 587
Bell E. F. et al., 2006a, ApJ, 640, 241
Bell E. F., Phleps S., Somerville R. S., Wolf C., Borch A., Meisenheimer K., 2006b, ApJ, in press (astro-ph/0602038)
Blake C. et al., 2004, MNRAS, 355, 713
Blanton M. R. et al., 2003, AJ, 125, 2348
Blanton M. R. et al., 2005, AJ, 129, 2562
Bohlin R. C., Jenkins E. B., Spitzer L., York D. G., Hill J. K., Savage B. D., Snow T. P., 1983, ApJS, 51, 277
Bower R. G., Lucey J. R., Ellis R. S., 1992, MNRAS, 254, 601
Bruzual G., Charlot S., 2003, MNRAS, 344, 1000 (BC03)
Cannon R. et al., 2006, MNRAS, 372, 425
Crawford C. S., Allen S. W., Ebeling H., Edge A. C., Fabian A. C., 1999, MNRAS, 306, 857

Cole S., Aragon-Salamanca A., Frenk C. S., Navarro J. F., Zepf S. E., 1994, MNRAS, 271, 781

Colless M. et al., 2001, MNRAS, 328, 1039

Collister A. et al., 2006, MNRAS, submitted

Couch W. J., Sharples R. M., 1987, MNRAS, 229, 423

De Lucia G., Springel V., White S. D. M., Croton D., Kauffmann G., 2006, MNRAS, 366, 499

Doherty M., Bunker A. J., Ellis R. S., McCarthy P. J., 2005, MNRAS, 361, 525

Donahue M., Stocke J. T., Gioia I. M., 1992, ApJ, 385, 49

Eisenstein D. J. et al., 2001, AJ, 122, 2267

Eisenstein D. J. et al., 2003, ApJ, 585, 694

Ellis R. S., Smail I., Dressler A., Couch W. J., Oemler A. J., Butcher H., Sharples R. M., 1997, ApJ, 483, 582

Fukugita M., Ichikawa T., Gunn J. E., Doi M., Shimasaku K., Schneider D. P., 1996, AJ, 111, 1748

Fukugita M., Nakamura O., Turner E. L., Helmboldt J., Nichol R. C., 2004, ApJ, 601, L127

Kauffmann G., Charlot S., 1998, MNRAS, 294, 705

Kennicutt R. C., 1992, ApJ, 388, 310

Kodama T., Arimoto N., Barger A. J., Arag'on-Salamanca A., 1998, A&A, 334, 99

Le Fèvre O. et al., 2000, MNRAS, 311, 565

Le Borgne D. et al., 2006, ApJ, 642, 48

Michard R., Prugniel P., 2004, A&A, 423, 833

Murali C., Katz N., Hernquist L., Weinberg D. H., Davé R., 2002, ApJ, 571, 1

Padmanabhan N., Budavári T., Schlegel D. J., Bridges T. et al., 2005, MNRAS, 359, 237

Pimbblet K. A., Smail I., Edge A. C., O'Hely E., Couch W. J., Zabludoff A. I., 2006, MNRAS, 366, 645

Poggianti B. M., Smail I., Dressler A., Couch W. J., Barger A. J., Butcher H., Ellis R. S., Oemler A. J., 1999, ApJ, 518, 576

Pracy M. B., Couch W. J., Blake C., Bekki K., Harrison C., Colless M., Kuntschner H., de Propris R., 2005, MNRAS, 359, 1421

Salpeter E. E., 1955, ApJ, 121, 161

Spergel D. N. et al., 2003, ApJS, 148, 175

Stanford S. A., Eisenhardt P. R., Dickinson M., 1998, ApJ, 492, 461

Stanford S. A., Eisenhardt P. R. M., Dickinson M., 1995, ApJ, 450, 512

Stoughton C. et al., 2002, AJ, 123, 485

Terlevich A. I., Caldwell N., Bower R. G., 2001, MNRAS, 326, 1547

van Dokkum P. G., 2005, AJ, 130, 2647

van Dokkum P. G., Franx M., 2001, ApJ, 553, 90

van Dokkum P. G., Stanford S. A., 2003, ApJ, 585, 78

Veilleux S., Osterbrock D. E., 1987, ApJS, 63, 295

Visvanathan N., Sandage A., 1977, ApJ, 216, 214

Wake D. A. et al., 2006, MNRAS, 372, 537

Willis J. P., Hewett P. C., Warren S. J., Lewis G. F., 2002, MNRAS, 337, 953

Worthey G., Ottaviani D. L., 1997, ApJS, 111, 377

Yi S. K. et al., 2005, ApJ, 619, L111

This paper has been typeset from a TeX/LaTeX file prepared by the author.